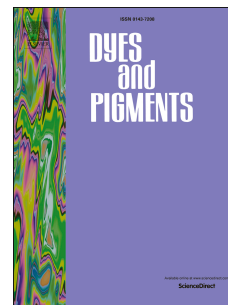


# Accepted Manuscript

A highly selective fluorescent sensor for Cd<sup>2+</sup> based on a new diarylethene with a 1,8-naphthyridine unit

Xiaoxia Zhang, Renjie Wang, Congbin Fan, Gang Liu, Shouzhi Pu



PII: S0143-7208(16)31058-0

DOI: [10.1016/j.dyepig.2016.12.023](https://doi.org/10.1016/j.dyepig.2016.12.023)

Reference: DYPI 5648

To appear in: *Dyes and Pigments*

Received Date: 26 October 2016

Revised Date: 7 December 2016

Accepted Date: 11 December 2016

Please cite this article as: Zhang X, Wang R, Fan C, Liu G, Pu S, A highly selective fluorescent sensor for Cd<sup>2+</sup> based on a new diarylethene with a 1,8-naphthyridine unit, *Dyes and Pigments* (2017), doi: 10.1016/j.dyepig.2016.12.023.

This is a PDF file of an unedited manuscript that has been accepted for publication. As a service to our customers we are providing this early version of the manuscript. The manuscript will undergo copyediting, typesetting, and review of the resulting proof before it is published in its final form. Please note that during the production process errors may be discovered which could affect the content, and all legal disclaimers that apply to the journal pertain.

# A highly selective fluorescent sensor for Cd<sup>2+</sup> based on a new diarylethene with a 1,8-naphthyridine unit

Xiaoxia Zhang,<sup>a</sup> Renjie Wang,<sup>ab\*</sup> Congbin Fan,<sup>a</sup> Gang Liu,<sup>a</sup> Shouzhi Pu<sup>a\*</sup>

<sup>a</sup> Jiangxi Key Laboratory of Organic Chemistry, Jiangxi Science and Technology Normal University,

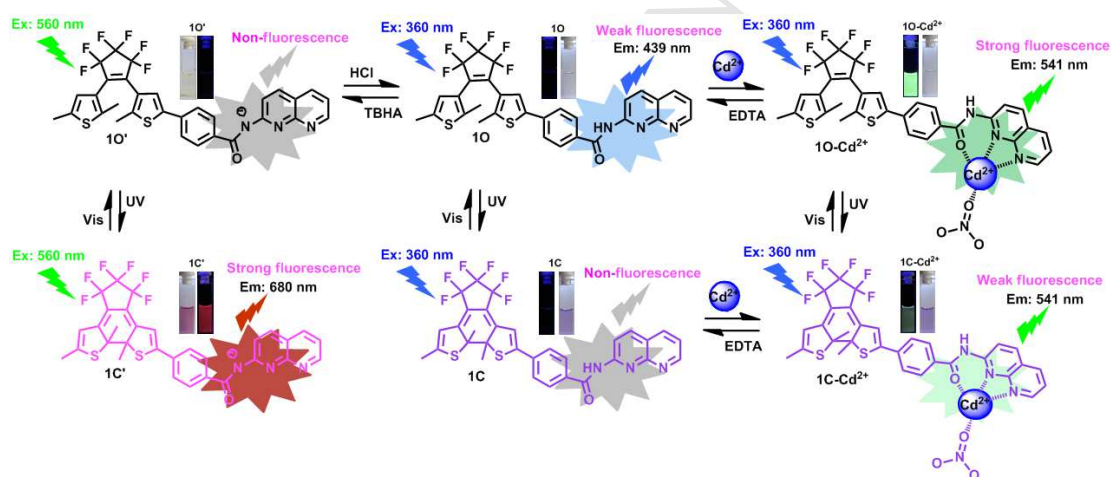
Nanchang 330013, P. R. China

<sup>b</sup> College of Chemistry, Nanchang University, Nanchang, Jiangxi 330031, P. R. China

\*Corresponding author 1: Tel.: +86-791-3831996; fax: +86-791-3831996; E-mail address:

[pushouzhi@tsinghua.org.cn](mailto:pushouzhi@tsinghua.org.cn) (S. Pu)

\*Corresponding author 2: Tel.: +86-791-88531582; E-mail address: [bio-wrj@163.com](mailto:bio-wrj@163.com) (R. Wang).



**Abstract:** A new asymmetrical photochromic diarylethene has been synthesized by using 1,8-naphthyridine as a functional group and perfluorodiarylethene as photoswitching unit via a peptide bond linkage, and its molecular structure was characterized by single crystal X-ray diffraction analysis. The compound exhibited favorable photochromism upon irradiation with UV/vis light, and its fluorescent behaviour could be efficiently modulated by light, base/acid, and metal ion in THF. The deprotonated derivative of the diarylethene also showed good photochromism, and displayed remarkable “turn-on” fluorescence response during photocyclization process. Furthermore, the diarylethene was highly selective toward  $\text{Cd}^{2+}$  with an obvious fluorescent color change from dark to bright green in THF. Finally, a logic circuit was fabricated with four inputs of the combinational stimuli of UV/vis and  $\text{Cd}^{2+}$ /EDTA, and one output of fluorescence intensity.

**Keywords:** Diarylethene; Photochromism; Fluorescent sensor;  $\text{Cd}^{2+}$  recognition; Logic circuit.

## Introduction

Compared with traditional analytical methods, such as ion selective electrodes, voltammetric methods and colorimetric sensors, the development of fluorescent chemosensors for sensing and recognition metal ions of importance to the environment and health has attracted considerable attention, due to their simplicity, high sensitivity, good selectivity and rapid response time [1-6]. Among various metal ions,  $\text{Cd}^{2+}$  has been recognized as a highly toxic heavy metal ion and widely used in many fields such as electroplating, metallurgy, weapons industry and agriculture [7-10]. Humans are chronically exposed to  $\text{Cd}^{2+}$  sources through the ingestion of contaminated food or water, which can easily lead to serious injury to the kidney, lung, bone, nervous system and even certain cancers [11-17]. Furthermore, compared with other metal cations, the detection of  $\text{Cd}^{2+}$  has always been a thorny problem because it is difficult to eliminate serious interference from  $\text{Zn}^{2+}$ , as they have similar physical and chemical properties [18-22]. To date, only a few highly selective fluorescent chemosensors for  $\text{Cd}^{2+}$  have been developed [14, 23].

Photochromism is a reversible transformation between two isomers with different absorption spectra in response to light stimuli, and has always attracted substantial attention for a wide range of applications as building blocks, molecular motors, photochromic lenses, nanoscale optical storage devices, multifunctional devices and logic circuits. Among various photochromic compounds, diarylethene derivatives have been well-recognized due to their excellent thermal stability, high photoisomerization quantum yields and remarkable fatigue resistance [24-31]. In recent years, many fluorescence chemosensors and multi-photoswitchable molecules based on diarylethenes have been designed and synthesized [32-34]. For example, Zeng and coworkers have reported a phenathrene-bridged terarylene with two crown ethers as ion recognizing moieties, which can

efficiently detect  $\text{Hg}^{2+}$  via the colorimetric sensing mechanism [35]. Tian *et. al* have exploited an asymmetric diarylethene with a *o*-amimophenol moiety to selectively recognize  $\text{Cu}^{2+}$  through inducing a change in fluorescence. Moreover, its fluorescence could further increase via the specific coordination of  $\text{CN}^-$  with the  $\text{Cu}^{2+}$  complex, and a complicated logic circuit with three inputs (UV,  $\text{Cu}^{2+}$ , and  $\text{CN}^-$ ) and three outputs ( $I \leq 100$ ,  $100 < I \leq 150$ , and  $I \geq 150$ ,  $I$  = fluorescence intensity at 448 nm) was developed using these characters [36]. In our previous work, various functional units (such as quinoline, phenanthroline, terpyridine and antipyrine) were introduced into diarylethenes, and most could serve as chemosensors for various metal ions ( $\text{Hg}^{2+}$ ,  $\text{Sn}^{2+}$ ,  $\text{Zn}^{2+}$  and  $\text{Al}^{3+}$ ) [37-40]. However, only few reports on diarylethene-based fluorescent chemosensors are for  $\text{Cd}^{2+}$  [41-43], because  $\text{Zn}^{2+}$ -induced interference in  $\text{Cd}^{2+}$  detection is difficult to eliminate [44-46].

1,8-Naphthyridine, a simple heterocycle with two ring nitrogens is well known for typical intramolecular charge transfer fluorophore, high photostability, large Stokes' shift and insensitivity to pH [47]. In recent years, 1,8-naphthyridine derivatives have also attracted much attention because they exhibit multi-functional biological activity [48-51]. The two edge-fused pyridine rings in 1,8-naphthyridine ligand have a constrained "bite" distance (2.2 Å), which is attributed to high coordinate architecture [52]. In addition, modifications of 1,8-naphthyridine have given rise to a great number of derivatives with tunable binding properties and a variety of fluorescent properties via chelating with ions (such as  $\text{Hg}^{2+}$ ,  $\text{Cu}^{2+}$ ,  $\text{Cr}^{3+}$  and  $\text{CN}^-$ ) [48,53-56]. However, fluorescent sensors based on diarylethene bearing a 1,8-naphthyridine unit for detecting  $\text{Cd}^{2+}$  have not hitherto been reported. On the basis of the mentioned facts, a new photochromic diarylethene fluorescence chemosensor bearing a 1,8-naphthyridine unit (**10**) with high selectivity for  $\text{Cd}^{2+}$  was constructed. The photochromic behaviour and multifunctional fluorescent switching characteristics of **10**

induced by light, acid/base, and metal ion were systematically studied and discussed. The schematic illustration of photochromism is shown in Scheme 1.

<Scheme 1>

## 2. Experimental

### 2.1. General methods

Unless otherwise stated, all of the materials for the synthesis of the target compound were purchased from various commercial sources and used without further purification. The solvents used were purified by standard methods prior to use. The solutions of metal ions ( $0.1 \text{ mol L}^{-1}$ ) were prepared by the dissolution of their respective metal nitrates in distilled water, except for  $\text{Mn}^{2+}$ ,  $\text{Hg}^{2+}$ ,  $\text{K}^+$ , and  $\text{Ba}^{2+}$  (their counterions were chloride ions). NMR spectra were recorded on a Bruker AV400 (400 MHz) spectrometer with  $\text{CDCl}_3$  as the solvent and tetramethylsilane as an internal standard. Infrared spectra (IR) were recorded on a Bruker Vertex-70 spectrophotometer. Melting point was measured on a WRS-1B melting point apparatus. Absorption spectra were measured using an Agilent 8453 UV/vis spectrophotometer. Photoirradiation was carried out using an MUL-165 UV lamp and a MVL-210 visible lamp. The required wavelength was isolated by the use of appropriate filters. Fluorescence spectra were measured using a Hitachi F-4600 spectrophotometer with 5 nm slit for both excitation and emission. Mass spectra were obtained on a Bruker AmaZon SL spectrometer. Elemental analysis was measured with a PE CHN 2400 analyzer. The fluorescence quantum yield was measured with an Absolute PL Quantum Yield Spectrometer QY C11347-11. The pH was measured with a PHS-3C analyzer. Crystal structure was solved through direct methods and refined through full-matrix least-squares procedures on  $F^2$  in SHELXTL-97 program. Further details on the crystal structure investigation have been deposited with The Cambridge Crystallographic

Data Centre as supplementary publication CCDC 1511213 for **10**. Copy of the data can be obtained, free of charge, on application to CCDC, 12 Union Road, Cambridge CB2 1EZ, UK (fax: +44 0 1223 336033 or e-mail:deposit@ccdc.cam.ac.uk).

<Scheme 2>

**2.2** **Synthesis** **of**  
**4-(4-(2-(2,5-dimethylthiophen-3-yl)-3,3,4,4,5,5-hexafluorocyclopent-1-en-1-yl)-5-methylthiophen-2-yl)-N-(1,8-naphthyridin-2-yl)benzamide 10**

The synthetic route for diarylethene **10** is shown in Scheme 2. The intermediate compounds **2** and **3** were synthesized according to the similar procedures as previous descriptions [57,58]. A mixture of compound **3** (0.56 g, 1.0 mmol), **4** (0.15 g, 1.0 mmol), EDCI (0.23 g, 1.2 mmol), HOBT (0.16 g, 1.2 mmol) and triethylamine (0.41 mL, 3.0 mmol) in anhydrous CH<sub>2</sub>Cl<sub>2</sub> (50 mL) was stirred at room temperature for 10 hours under a nitrogen atmosphere. The reaction mixture was washed with water, dried over anhydrous Na<sub>2</sub>SO<sub>4</sub>, and evaporated. The crude product was purified by column chromatography using petroleum ether/ethyl acetate (v/v = 1:1) as eluent to obtain 0.15 g of the target compound **10** as white solid in 24% yield. M.p. 504–505 K; <sup>1</sup>H NMR (400 MHz, THF, ppm): δ 1.82 (s, 3H), 1.89 (s, 3H), 2.32 (s, 3H), 6.71 (s, 1H), 7.27–7.30 (m, 1H), 7.46 (s, 1H), 7.67 (d, 2H, *J* = 8.0 Hz), 8.07 (d, 2H, *J* = 8.0 Hz), 8.12 (d, 1H, *J* = 8.0 Hz), 8.20 (d, 1H, *J* = 8.0 Hz), 8.52 (d, 1H, *J* = 8.0 Hz), 8.84 (s, 1H), 10.45 (s, 1H); <sup>13</sup>C NMR (100 MHz, THF, ppm): δ 11.50, 11.62, 12.01, 113.63, 118.49, 118.70, 122.10, 122.44, 122.73, 123.19, 124.37, 126.98, 131.74, 134.40, 134.77, 136.38, 136.93, 138.13, 139.25, 140.62, 151.42, 152.96, 153.39, 163.66; IR (KBr, ν, cm<sup>-1</sup>): 712, 735, 759, 783, 809, 825, 843, 890, 937, 988, 1050, 1102, 1138, 1187, 1264, 1275, 1336, 1424, 1493, 1608, 1674, 2860, 2928, 3217, 3517; Anal. Calcd for C<sub>31</sub>H<sub>21</sub>F<sub>6</sub>N<sub>3</sub>OS<sub>2</sub>: C, 59.13; H, 3.36; N, 6.67;

found: C, 59.04; H, 3.41; N, 6.59; HRMS-ESI ( $m/z$ ):  $[M + Na^+]^+$  calcd. 652.0928, found: 652.0901.

### 3. Results and discussion

#### 3.1 Photochromic and fluorescent properties

##### <Figure 1>

The photochromic behavior of diarylethene **10** induced by UV/vis light was investigated in THF solution ( $C = 2.0 \times 10^{-5} \text{ mol L}^{-1}$ ) at room temperature. As shown in Figure 1, the open-ring isomer **10** exhibited a sharp absorption peak at 331 nm ( $\epsilon = 3.62 \times 10^4 \text{ L mol}^{-1} \text{ cm}^{-1}$ ) due to  $\pi \rightarrow \pi^*$  transition [56]. Upon irradiation with 313 nm light, a new visible absorption band centered at 562 nm ( $\epsilon = 9.31 \times 10^3 \text{ L mol}^{-1} \text{ cm}^{-1}$ ) emerged while the original peak at 331 nm decreased due to the formation of the closed-ring isomer **1C**, accompanied with the colorless solution becoming purple. Alternatively, the purple solution could be completely bleached upon illumination with visible light ( $\lambda > 450 \text{ nm}$ ). After irradiating with 313 nm light for 10 min, the photostationary state (PSS) of **1** was arrived and a clear isosbestic point was observed at 353 nm, which supported the reversible two-component photochromic reaction [59,60]. In addition, the photoconversion ratio from open-ring to closed-ring isomer of **1** was analyzed by  $^1\text{H NMR}$  in PSS, and the conversion value was determined as 48 %. The cyclization and cycloreversion quantum yields of **1** were determined in THF by using 1,2-bis(2-methyl-5-phenyl-3-thienyl)perfluorocyclopentene as a reference, and the values were measured as 0.18 and 0.10, respectively.

##### <Figure 2>

In order to observe molecular conformation and evaluate the photochromic reactivity in the crystal, X-ray crystallographic analysis was carried out. The single crystal of **1** was obtained by slow evaporation of methanol solution. Table S1 shows crystallographic data for **10**, which belonged to

space groups of Triclinic *P*-1 and contain a molecule of water. The crystal density of **10** was determined to be 1.442 g cm<sup>-3</sup>. Table S2 lists the corresponding dihedral angles and distances between the reactive carbon atoms. For **10**, the dihedral angles between the hexafluorocyclopentene ring and the heteroaryl ring [thiophene ring (S2) and thiophene ring (S1)] are 46.7° for S2/C26-C27-C29-C30 and 41.5° S1/C16- C17-C18-C19. The dihedral angle between the thiophene ring (S1) and its adjacent benzene ring is 20.5°. Notably, the dihedral angle between the benzene ring and the naphthyridine is 1.6°, indicating the two rings are near coplanarity. Figure 2A shows the molecular structure of **1** in the crystal. It can be clearly seen that **10** molecule adopts a photoreactive anti-parallel conformation. The double bond (C21–C25) of the hexafluorocyclopentene ring is 1.355 Å, which is significantly shorter than other carbon-carbon single bonds (1.503 Å to 1.517 Å) of the central ring. The intramolecular distance between the two reactive carbon atoms (C19–C27) is 3.573 Å. Therefore, the conformation and the distance fulfill the requirement for diarylethene molecule to undergo photocyclization reaction in the single crystalline phase [61]. Upon irradiation with UV light ( $\lambda = 365$  nm), the light yellow single crystal of **10** quickly turned to blue due to the formation of the closed-ring isomer **1C**. Conversely, irradiation of visible light ( $\lambda > 450$  nm) completely erased the blue color of the crystal, indicating that the process was reversible (Figure. 2B).

<Figure 3>

Like most other reported diarylethenes [62,63], **10** exhibited fluorescence switching characteristics upon alternating irradiation of UV and visible light. Figure 3 shows the emission spectral changes of **10** upon photoirradiation when excited at 360 nm light. The fluorescence emission peak of **10** was observed at 439 nm in THF, and the absolute fluorescence quantum yield was determined to be

0.003. Upon irradiation with 313 nm UV light, the emission intensity of **10** gradually decreased due to the formation of non-fluorescence closed-ring isomer **1C**. The back irradiation with appropriate visible light ( $\lambda > 450$  nm) regenerated the open-ring isomer **10**, and recovered the original emission intensity. In the PSS, the fluorescence intensity of **10** was quenched to *ca.* 35%. The residual fluorescence in the photostationary state may be attributed to the incomplete cyclization and the existence of isomers with parallel conformation.

### 3.2 Changes in absorption and fluorescence by base/acid stimuli

#### <Figure 4>

Just as the reported diarylethenes [38,64], diarylethene **1** also exhibited multi-responsive characteristic upon stimulation with base/acid and UV/vis light. The absorption spectral changes of **10** induced by tetrabutyl ammonium hydroxide (TBAH) and hydrochloric acid (HCl) in THF were measured at room temperature and shown in Figure 4A. When TBAH solution was added to the colorless solution of **10**, the absorption maximum at 331 nm gradually decreased and a new absorption band was observed at 387 nm due to the formation of deprotonated diarylethene **10'**. This change could be easily seen visually, as the colourless solution of **10** became pale yellow. In an absorption titration experiment, the absorption intensity of **10'** at 387 nm was enhanced accompanied with the TBAH concentration increased from 0 to 20.0 equiv (8.0  $\mu\text{L}$ , 0.1 mol L<sup>-1</sup>), followed by a plateau with further titration (Figure S1, SI). Reversely, **10'** could be neutralized with 20.0 equiv HCl (8.0  $\mu\text{L}$ , 0.1 mol L<sup>-1</sup>) and recover the absorption spectrum of **10**. Notably, **10'** also could undergo reversible photoisomerization (Figure 4B). Upon irradiation with 313 nm light, the pale yellow solution of **10'** turned to magenta and a new obvious visible absorption band was observed at 550 nm ( $\epsilon = 2.81 \times 10^4$  L mol<sup>-1</sup> cm<sup>-1</sup>) due to the formation of the closed-ring isomer **1C'**.

The magenta solution could be thoroughly reverted to pale yellow upon irradiation with visible light ( $\lambda > 450$  nm), indicating the original open-ring isomer **10'** was restored. The cyclization and cycloreversion quantum yields of **1'** were measured to be 0.27 and 0.005 (Table 1). Compared with **1**, the molar absorption coefficient (**1C'**,  $\varepsilon = 2.81 \times 10^4$ ) and the cyclization quantum yields ( $\Phi_{1', o-c} = 0.27$ ) exhibited notable enhancement, while the cycloreversion quantum yields ( $\Phi_{1', c-o} = 0.005$ ) distinctly decreased. The result indicated that the deprotonation effect could efficiently promote the photocyclization reaction and heavily suppress the photocycloreversion reaction of **1**. The structures and color changes of **1'** induced by base/acid and UV/vis light are illustrated in Scheme 3. Moreover, the reversible transformation between **1C** and **1C'** could be realized by the stimulation of TBAH and HCl (Figure 4C). After adding 21.0 equiv (8.4  $\mu\text{L}$ ,  $0.1 \text{ mol L}^{-1}$ ) TBAH to the purple solution of **1C**, the color changed to magenta and the absorption intensity notably enhanced with a obvious blue-shifted from 562 nm to 550 nm due to the formation of the deprotonated **1C'**, which could also return to **10** by stimulation with 21.0 equiv of HCl (8.4  $\mu\text{L}$ ,  $0.1 \text{ mol L}^{-1}$ ).

<Table 1>

<Scheme 3>

Notably, the deprotonation effect not only influenced the absorption spectra of **1** but also heavily affected the fluorescence properties. Like the open-ring isomer of **10**, **10'** also showed very weak fluorescence in THF solution when excited at 360 nm light. However, the closed-ring isomer **1C'** exhibited brilliant red fluorescence at around 678 nm when excited at 560 nm light. After reaching the PSS, the intensity of **10** was enhanced 135 fold (Figure 5), and the fluorescence quantum yield of **1C'** was determined to be 0.061 in THF through using an Absolute PL Quantum Yield Spectrometer QY C11347-11. The photoinduced electron transfer and the high coplanarity of the

closed-ring isomer (**1C'**) may be responsible for this phenomenon. On the one side, the deprotonation effect may interfere the electron transfer from 1,8-naphthyridine group to the diarylethene, and block the photoinduced electron transfer (PET) process [18,65], which may induce the fluorescence of **1C'** notable enhancement. On the other side, the structure of hexadiene in the closed-ring isomer **1C'** had much higher coplanarity than the open-ring isomer **1O'** [24,66,67], and the benzene ring and the 1,8-naphthyridine ring were near coplanarity. Therefore, the molecular structure of **1C'** displayed a high coplanarity, which further induced the fluorescence enhancement effect. The result was completely contrary to that reported for a diarylethene with a salicylidene Schiff base substituent, in which the deprotonated closed-ring isomer exhibited non-fluorescence, while the open-ring isomer showed strong fluorescence emission and bright orange emission [68]. Back irradiation by appropriate visible light ( $\lambda > 450$  nm) regenerated the open-ring isomers **1O'**, and recovered the original emission intensity. Therefore, the switching behavior of the deprotonation diarylethene (**1O'**) is a promising candidate for potential application in "turn-on" photoswitchable devices.

<Figure 5>

### 3.3 Fluorescence response to metal ions

<Figure 6>

The fluorescence changes of diarylethene **1** induced by addition of various metal ions in THF was investigated at room temperature. Figure 6 shows the emission spectra and fluorescence color changes of **1O** induced by the addition of various metal ions (3.0 equiv), including  $\text{Fe}^{3+}$ ,  $\text{Sr}^{2+}$ ,  $\text{Co}^{2+}$ ,  $\text{Ni}^{2+}$ ,  $\text{Mn}^{2+}$ ,  $\text{Ba}^{2+}$ ,  $\text{Pb}^{2+}$ ,  $\text{Hg}^{2+}$ ,  $\text{Ca}^{2+}$ ,  $\text{Mg}^{2+}$ ,  $\text{Sn}^{2+}$ ,  $\text{Cd}^{2+}$ ,  $\text{Zn}^{2+}$ ,  $\text{Al}^{3+}$ ,  $\text{Cr}^{3+}$ ,  $\text{Cu}^{2+}$ ,  $\text{K}^+$  and  $\text{Ag}^+$  in THF ( $2.0 \times 10^{-5}$  mol  $\text{L}^{-1}$ ), respectively. It could be seen that none of these ions induced any significant

changes in the fluorescence spectrum of **10** except for  $\text{Cd}^{2+}$ ,  $\text{Ag}^+$ , and  $\text{Zn}^{2+}$ . Compared to  $\text{Cd}^{2+}$ , the fluorescence emission intensity of **10** exhibited minor change with the addition of the same amount of  $\text{Ag}^+$  and  $\text{Zn}^{2+}$ . The results indicated that the binding ability of  $\text{Cd}^{2+}$  with diarylethene **1** was higher than that of other metal ions. Additionally, in order to elucidate the response time of  $\text{Cd}^{2+}$  to **10**, the relationship curve between the duration time of  $\text{Cd}^{2+}$  and emission intensity change of **10** were carried out. Figure S2 (SI) shows the emission intensity of **10** as a function of time in the presence of 3.0 equiv of  $\text{Cd}^{2+}$  in THF. It could be easily seen that the fluorescence intensity of **10** showed no obvious change during prolonging the time from 0 to 30 min. The results indicated that the fluorescence of **10** in response to  $\text{Cd}^{2+}$  was independent to time.

Figure 7A shows the fluorometric titration profile of **1** with  $\text{Cd}^{2+}$ . Upon gradual addition of  $\text{Cd}^{2+}$  to the solution of **1**, the original weak fluorescence signal in the range of 400–500 nm was remarkably red-shifted to 541 nm with a marked enhancement in fluorescence intensity. Upon excitation at 360 nm, a concomitant color change from dark to bright green was observed due to the formation of the complex **10**- $\text{Cd}^{2+}$ . When the concentration of  $\text{Cd}^{2+}$  increased to 3.0 equiv, the fluorescence intensity of **10**- $\text{Cd}^{2+}$  at 541 nm reached a plateau. There was a good linearity between the concentration of  $\text{Cd}^{2+}$  (0  $\rightarrow$  3.0 equiv) and the ratio of the fluorescence intensities ( $I_{541 \text{ nm}}/I_{439 \text{ nm}}$ ) (Figure S3, SI), demonstrating that diarylethene **1** could quantitatively detect  $\text{Cd}^{2+}$  at the relevant concentration. In addition, the binding constant ( $K_a$ ) of **10** with  $\text{Cd}^{2+}$  was determined to be  $8.60 \times 10^3 \text{ L mol}^{-1}$  with good linear relationship ( $R = 0.998$ , Figure S4, SI), as obtained by fitting the data to the Benesi-Hildebrand expression [69]. Meanwhile, the absolute fluorescence quantum yield of **10**- $\text{Cd}^{2+}$  was determined to be 0.039. After EDTA was added to **10**- $\text{Cd}^{2+}$ , the fluorescence of **10** was restored. The result was attributed to the complexation-dissociation reaction between  $\text{Cd}^{2+}$  and

EDTA. Moreover, the complex **10**-Cd<sup>2+</sup> exhibited a notable fluorescence switch by photoirradiation (Figure 7B). Upon irradiation with 313 nm light, the emission intensity of **10**-Cd<sup>2+</sup> was quenched to *ca.* 87% due to the formation of the non-fluorescence **1C**-Cd<sup>2+</sup> when arrived at the PSS. Alternatively, the back irradiation with appropriate visible light regenerated the open-ring isomer **10**-Cd<sup>2+</sup> and recovered its original emission intensity. Therefore, dual-controlled photoswitching circulation behavior of **10** induced by Cd<sup>2+</sup>/EDTA and UV/vis light stimuli could be constructed (Scheme 4). Furthermore, in order to check the suitable pH range for Cd<sup>2+</sup> detection, the pH effect on the complexation of **10** with Cd<sup>2+</sup> were carried out at room temperature. When pH was increased from 2.0 to 7.5, the fluorescence emission intensity of **10** gradually enhanced with the addition of 3.0 equiv Cd<sup>2+</sup>. The emission intensity showed slowly decreased and arrived at a plateau with the increase of pH value from 7.5 to 13.5 (Figure S5, SI). The results indicated that **10** could be used as a good Cd<sup>2+</sup> probe even in acid and base environment.

<Figure 7>

<Scheme 4>

Subsequently, a competitive experiment was carried out by adding Cd<sup>2+</sup> to the solution of **10** in the presence of other metal ions, and the results was shown in Figure 8A. Before the introduction of Cd<sup>2+</sup>, there were almost no fluorescence changes at 541 nm in the presence of other metal ions. When 3.0 equiv Cd<sup>2+</sup> was introduced to the above mentioned solution, a notable fluorescence enhancement effect at 541 nm was observed. The results clearly demonstrated any metal ions considered in the study did not interfere with the detection of Cd<sup>2+</sup>. In order to understand the binding stoichiometry of **10**-Cd<sup>2+</sup>, Job's plot experiment was performed. As shown in Figure 8B, the emission intensity at 541 nm was plotted as a function of the mole fraction of **1** under a constant

total concentration. The concentration of the complex **10**-Cd<sup>2+</sup> approached the maximum value when the molar fraction of  $[\mathbf{10}]/([\mathbf{10}]+[\text{Cd}^{2+}])$  was 0.5, suggesting that a 1:1 binding stoichiometry ratio for **10**-Cd<sup>2+</sup> complex. To further confirm **10** binding form with Cd<sup>2+</sup>, the <sup>1</sup>H NMR titration experiment in THF-*d*<sub>8</sub> was performed. The chemical shift of the amide NH can be used to distinguish whether Cd<sup>2+</sup> is bound to carbonyl oxygen or imidic acid nitrogen [70]. As shown in Figure 8C, the chemical shift of the amine NH exhibited resonance upfield with the addition of Cd<sup>2+</sup> increased from 0 to 1.0 equiv. The results indicated that the carbonyl oxygen was participated in the complexation with Cd<sup>2+</sup> because the Cd<sup>2+</sup> blocked the amide resonance and induced the NH resonance upfield. The H<sub>b-e</sub> protons showed downfield shifts in THF-*d*<sub>8</sub> (H<sub>b</sub> 8.08→8.36; H<sub>c</sub> 8.14→8.50; H<sub>d</sub> 8.84→8.87, and H<sub>e</sub> 7.30→7.57), indicating that Cd<sup>2+</sup> coordinated with two naphthyridine nitrogen-atoms. Furthermore, the formation of **10**-Cd<sup>2+</sup> complex was confirmed by using ESI-MS in which the peak at  $m/z = 804.8$  for  $[\mathbf{1} + \text{Cd}^{2+} + \text{NO}_3]^{+}$  (Figure S6, SI). The result indicated that **10** bound to Cd<sup>2+</sup> with a binding stoichiometry of 1:1. The binding mechanism between **10** and Cd<sup>2+</sup> is shown in Scheme 4. Moreover, to determine the limit of detection of **10** toward Cd<sup>2+</sup>, we recorded the fluorescence data starting from the Cd<sup>2+</sup> concentration as low as 10<sup>-9</sup> M using 0.04 μM solution of **10** (Figure S7, SI). From the concentration-dependent fluorescence titration experiment, the detection limit of **10** was found to be 1.97 × 10<sup>-7</sup> mol L<sup>-1</sup> for Cd<sup>2+</sup>, by the reported method [71].

<Figure 8>

### 3.4 Application as a logic circuit

As mentioned above, the fluorescence of **10** could be independently modulated by the stimulation of UV/vis light and Cd<sup>2+</sup> / EDTA. On the basis of this fact, a combinational logic circuit by the

stimulation of light irradiation (In1: 313 nm light and In2:  $\lambda > 450$  nm visible light) and chemical species (In3:  $\text{Cd}^{2+}$  and In4: EDTA) as input signals and the change of fluorescence intensity at 541nm as output signal (Figure 9) were constructed. The emission intensity of **10** at 541 nm was regarded as an initial. When the emission intensity at 541 nm was 3-fold larger than the initial value, the output signal could be regarded as 'on' state with a Boolean value of '1'; Otherwise, it was regarded as 'off' state with a Boolean value of '0'. Under the stimuli of different inputs, the diarylethene showed an 'on' - 'off' - 'on' fluorescence switching behavior. Consequently, **10** could read a string of four inputs and write one output. For example, when the string is '0, 0, 1, and 0' the corresponding input signals of In1, In2, In3, and In4 are 'off, off, on, and off'. Under these conditions, **10** was converted to **10**- $\text{Cd}^{2+}$  by the stimulation of  $\text{Cd}^{2+}$  and its emission intensity enhanced dramatically. As a result, the output signal is 'on' and the output digit is '1'. Similarly, other stimulations also resulted in the same 'on' - 'off' - 'on' fluorescence switch and all possible logic strings were concluded in the combinational logic circuit as shown in Table 2.

<Figure 9>

<Table 2>

#### 4. Conclusions

In summary, a novel fluorescent sensor based on a photochromic diarylethene with a 1,8-naphthyridine unit was developed, and it exhibited multi-responsive behaviour when triggered by light, acid/base, and  $\text{Cd}^{2+}$ . The deprotonated derivative not only showed excellent photochromic performance but also displayed notable near infrared fluorescence emission during the photocyclization. In addition, the diarylethene could be utilized as a fluorescent sensor for detection of  $\text{Cd}^{2+}$  with high selectivity, and a logic circuit was constructed on the basis of the unimolecular

platform. This work provides a useful design strategy for the construction of diarylthene-based fluorescent chemosensor for the recognition of specific metal ions with a certain functionalized group.

### Acknowledgements

This work was supported by the National Natural Science Foundation of China (51373072, 21362013 and 21262015), the Project of Jiangxi Advantage Sci-Tech Innovative Team (20142BCB24012), the Science Funds of Natural Science Foundation of Jiangxi Province (20132BAB203005), and the Masters' Innovative Foundation of Jiangxi Science and Technology Normal University (YC2014-X03).

### References

- [1] Hu Y, Li QQ, Li H, Guo QN, Lu YG, Li Z. A novel class of Cd(II), Hg(II) turn-on and Cu(II), Zn(II) turn-off Schiff base fluorescent probes. *Dalton Trans* 2010;39:11344-52.
- [2] Qin WW, Dou W, Leen V, Dehaen W, Auweraer MVD, Boens N. A ratiometric, fluorescent BODIPY-based probe for transition and heavy metal ions. *RSC Adv* 2016;6:7806-16.
- [3] Sun X, Wang YW, Peng Y. A selective and ratiometric bifunctional fluorescent probe for Al<sup>3+</sup> ion and proton. *Org Lett* 2012;14:3420-3.
- [4] Sen B, Mukherjee M, Banerjee S, Pal SA, Chattopadhyay, P. A rhodamine-based 'turn-on' Al<sup>3+</sup> ion-selective reporter and the resultant complex as a secondary sensor for F<sup>-</sup> ion are applicable to living cell staining. *Dalton Trans* 2015;44:8708-17.
- [5] Qin JC, Fan L, Wang BD, Yang ZY, Li TR. The design of a simple fluorescent chemosensor for Al<sup>3+</sup>/Zn<sup>2+</sup> via two different approaches. *Anal Methods* 2015;7:716-22.
- [6] Lin Q, Lu TT, Zhu X, Wei TB, Li H, Zhang YM. Rationally introduce multi-competitive

- binding interactions in supramolecular gels: a simple and efficient approach to develop multi-analyte sensor array. *Chem Sci* 2016;7:5341-5346.
- [7] Hao JN, Yan B. A water-stable lanthanide-functionalized MOF as a highly selective and sensitive fluorescent probe for  $\text{Cd}^{2+}$ . *Chem Commun* 2015;51:7737-40.
- [8] Lv Y, Wu L, Shen W, Wang J, Xuan G, Sun X. A porphyrin-based chemosensor for colorimetric and fluorometric detection of cadmium(II) with high selectivity. *J Porphyr Phthaloc* 2015;19:769-74.
- [9] Miao Q, Wu Z, Hai Z, Tao C, Yuan Q, Gong Y, et al. Bipyridine hydrogel for selective and visible detection and absorption of  $\text{Cd}^{2+}$ . *Nanoscale* 2015;7:2797-804.
- [10] Peng X, Du J, Fan J, Wang J, Wu Y, Zhao J, et al. A selective fluorescent sensor for imaging  $\text{Cd}^{2+}$  in living cells. *J Am Chem Soc* 2007;129:1500-1.
- [11] Kar C, Samanta S, Goswami S, Ramesh A, Das G, et al. A single probe to sense Al(III) colorimetrically and Cd(II) by turn-on fluorescence in physiological conditions and live cells, corroborated by X-ray crystallographic and theoretical studies. *Dalton Trans* 2015;44:4123-32.
- [12] Xu XY, Yan B. Eu(III) functionalized Zr-based metal-organic framework as excellent fluorescent probe for  $\text{Cd}^{2+}$  detection in aqueous environment. *Sens Actuators B* 2016;222:347-53.
- [13] Aich K, Goswami S, Das S, Mukhopadhyay CD, Quah CK, Fun HK.  $\text{Cd}^{2+}$  Triggered the FRET "ON": A new molecular switch for the ratiometric detection of  $\text{Cd}^{2+}$  with live-cell imaging and bound X-ray structure. *Inorg Chem* 2015;54:7309-15.
- [14] Luo Y, Tang D, Zhu W, Xu Y, Qian X. Reactive fluorescent dye functionalized cotton fabric as a "Magic Cloth" for selective sensing and reversible separation of  $\text{Cd}^{2+}$  in water. *J Mater Chem*

C 2015;3:8485-9.

- [15] Mehta VN, Rohit JV, Kailasa SK. Functionalization of silver nanoparticles with 5-sulfoanthranilic acid dithiocarbamate for selective colorimetric detection of  $Mn^{2+}$  and  $Cd^{2+}$  ions. *New J Chem* 2016;40:4566-74.
- [16] Park SY, Yoon JH, Hong CS, Souane R, Kim JS, Matthews SE, et al. A pyrenyl-appended triazole-based calix [4] arene as a fluorescent sensor for  $Cd^{2+}$  and  $Zn^{2+}$ . *J Org Chem* 2008;73:8212-8.
- [17] Liu W, Xu L, Sheng R, Wang P, Li H, Wu S. A water-soluble “switching on” fluorescent chemosensor of selectivity to  $Cd^{2+}$ . *Org Lett* 2007;9:3829-32.
- [18] Sil A, Maity A, Giri D, Patra SK. A phenylene–vinylene terpyridine conjugate fluorescent probe for distinguishing  $Cd^{2+}$  from  $Zn^{2+}$  with high sensitivity and selectivity. *Sens Actuators B* 2016;226:403-11.
- [19] Zhang L, Hu W, Yu L, Wang, Y. Click synthesis of a novel triazole bridged AIE active cyclodextrin probe for specific detection of  $Cd^{2+}$ . *Chem Commun* 2015;51:4298-301.
- [20] Xue L, Liu Q, Jiang H. Ratiometric  $Zn^{2+}$  fluorescent sensor and new approach for sensing  $Cd^{2+}$  by ratiometric displacement. *Org Lett* 2009;11:3454-7.
- [21] Qu WJ, Guan J, Wei TB, Yan G T, Lin Q, Zhang YM. A turn-on fluorescent sensor for relay recognition of two ions: from a  $F^{-}$ -selective sensor to highly  $Zn^{2+}$ -selective sensor by tuning electronic effects. *RSC Adv* 2016;6:35804-8.
- [22] Lin Q, Lu TT, Lou JC, Wu GY, Wei TB, Zhang YM. A “keto–enol tautomerization”-based response mechanism: a novel approach to stimuli-responsive supramolecular gel. *Chem Commun* 2015;51:12224-7.

- [23] Jiao SY, Li K, Zhang W, Liu YH, Huang Z, Yu, XQ. Cd(II)-terpyridine-based complex as a ratiometric fluorescent probe for pyrophosphate detection in solution and as an imaging agent in living cells. *Dalton Trans* 2015;44:1358-65.
- [24] Irie M, Fukaminato T, Matsuda K, Kobatake S. Photochromism of diarylethene molecules and crystals: memories, switches, and actuators. *Chem Rev* 2014; 114:12174-277.
- [25] Zhang JJ, Zou Q, Tian H. Photochromic materials: more than meets the eye. *Adv Mater* 2013;25:378-99.
- [26] Tian H, Yang SJ. Recent progresses on diarylethene based photochromic switches. *Chem Soc Rev* 2004;33:85-97.
- [27] Irie M. Diarylethenes for memories and switches. *Chem Rev* 2000;100:1685-716.
- [28] Fihey A, Perrier A, Browne WR, Jacquemin D. Multiphotochromic molecular systems. *Chem Soc Rev* 2015;44:3719-59.
- [29] Herder M, Schmidt BM, Grubert L, Pätzelt M, Schwarz J, Hecht S. Improving the fatigue resistance of diarylethene switches. *J Am Chem Soc* 2015;137:2738-47.
- [30] Takeshita T, Hara M. Resonance photoionization of a diarylethene derivative in the presence of cyclodextrins using multi-color multi-laser irradiation. *J Photochem Photobiol A* 2015;310:180-8.
- [31] Yin J, Lin Y, Cao XF, Yu GA, Tu HY, Liu SH. The synthesis and photochromic properties of two bis(phosphine) ligands based on dithienylethene backbone and their oxides, sulfurets and selenides. *Dyes Pigm* 2009;81:152-5.
- [32] Liu W, Hu F, Chen Z, Li Z, Yin J, Yu G, et al. Dithienylethenes containing aromatic carbons: Synthesis, photochromism and anion recognition *Dyes Pigm* 2015;115:190-6.

- [33] Zhang J, Jin J, Zou L, Tian H. Reversible photo-controllable gels based on bithienylethene-doped lecithin micelles. *Chem Commun* 2013;49:9926-8.
- [34] Li Z, Zhang C, Ren Y, Yin J, Liu, SH. Amide-and urea-functionalized dithienylethene: synthesis, photochromism, and binding with halide anions. *Org Lett* 2011;22:6022-5.
- [35] He J, He J, Wang T, Zeng H. Ion-induced cycle opening of a diarylethene and its application on visual detection of  $\text{Cu}^{2+}$  and  $\text{Hg}^{2+}$  and keypad lock. *J Mater Chem C* 2014;2:7531-40.
- [36] Zou Q, Li X, Zhang J, Zhou J, Sun B, Tian, H. Unsymmetrical diarylethenes as molecular keypad locks with tunable photochromism and fluorescence via  $\text{Cu}^{2+}$  and  $\text{CN}^-$  coordinations. *Chem Commun* 2012;48:2095-7.
- [37] Xia SJ, Liu G, Pu SZ. A highly selective fluorescence sensor for  $\text{Zn}^{2+}$  and  $\text{Cu}^{2+}$  based on diarylethene with a piperazine-linked amidopyridine unit. *J Mater Chem C* 2015;3:4023-9.
- [38] Pu SZ, Zhang CC, Fan CB, Liu G. Multi-controllable properties of an antipyrine-based diarylethene and its high selectivity for recognition of  $\text{Al}^{3+}$ . *Dyes Pigm* 2016;129:24-33.
- [39] Jia HJ, Pu SZ, Fan CB, Liu G, Zheng CH. A highly selective ratiometric fluorescent  $\text{Cu}^{2+}$  and  $\text{HSO}_4^-$  probe based on a new photochromic diarylethene with a 6-aryl[1,2-c]quinazoline unit. *Dyes Pigm* 2015;121:211-20.
- [40] Fu YL, Tu YY, Fan CB, Zheng CH, Liu G, Pu SZ. A highly sensitive fluorescent sensor for  $\text{Al}^{3+}$  and  $\text{Zn}^{2+}$  based on a diarylethene salicylhydrazide Schiff base derivative and its bioimaging in live cells. *New J Chem* 2016;40: 8579-86.
- [41] Ding HC, Liu G, Pu SZ, Zheng CH. Multi-addressable fluorescent switch based on a photochromic diarylethene with triazole-bridged methylquinoline group. *Dyes Pigm* 2014;103:82-8.

- [42] Liao GM, Zheng CH, Pu SZ. A highly selective fluorescent chemosensor for  $\text{Cd}^{2+}$  based on a new diarylethene with a pyridine-linked methylquinoline unit. *J Photochem Photobiol A* 2016;317:115-24.
- [43] Duan F, Liu G, Liu P, Fan CB, Pu SZ. A fluorescent probe for  $\text{Cd}^{2+}$  based on a diarylethene with pyridinepiperazine-linked hydroxyquinoline group. *Tetrahedron* 2016;72:3213-20.
- [44] Komatsu K, Kikuchi K, Kojima H, Urano Y, Nagano T. Selective zinc sensor molecules with various affinities for  $\text{Zn}^{2+}$ , revealing dynamics and regional distribution of synaptically released  $\text{Zn}^{2+}$  in hippocampal slices. *J Am Chem Soc* 2005;127:10197-204.
- [45] Nolan EM, Ryu JW, Jaworski J, Feazell RP, Sheng M, Lippard SJ. Zinspy sensors with enhanced dynamic range for imaging neuronal cell zinc uptake and mobilization. *J Am Chem Soc* 2006;128:15517-28.
- [46] Xue L, Li GP, Liu Q, Wang HH, Liu C, Ding XL, et al. Ratiometric fluorescent sensor based on inhibition of resonance for detection of cadmium in aqueous solution and living cells. *Inorg Chem* 2011;50:3680-90.
- [47] Qian X, Xiao Y, Xu Y, Guo X, Qian J, Zhu W. "Alive" dyes as fluorescent sensors: fluorophore, mechanism, receptor and images in living cells. *Chem Commun* 2010;46:6418-36.
- [48] Nicoletti CR, Garcia DN, Da Silva L, Begnini IM, Rebelo RA, Joussef AC, et al. Synthesis of 1,8-naphthyridines and their application in the development of anionic fluorogenic chemosensors. *J Fluoresc* 2012;22:1033-46.
- [49] Sato Y, Nishizawa S, Yoshimoto K, Seino T, Ichihashi, T, Morita, K, et al. Influence of substituent modifications on the binding of 2-amino-1,8-naphthyridines to cytosine opposite an AP site in DNA duplexes: thermodynamic characterization. *Nucleic Acids Res*

2009;37:1411-22.

- [50] Zhang HM, Fu WF, Gan X, Xu YQ, Wang J, Xu QQ, et al. A flexible 1,8-naphthyridyl derivative and its Zn(II) complexes: synthesis, structures, spectroscopic properties and recognition of Cd(II). *Dalton Trans* 2008;47:6817-24.
- [51] Morita K, Sato Y, Seino T, Nishizawa S, Teramae N. Fluorescence and electrochemical detection of pyrimidine/purine transversion by a ferrocenyl aminonaphthyridine derivative. *Org Biomol Chem* 2008;6:266-8.
- [52] Bera JK, Sadhukhan N, Majumdar M. 1,8-naphthyridine revisited: Applications in dimetal chemistry. *Eur J Inorg Chem* 2009;2009:4023-38.
- [53] Shi YG, Duan YL, Chen JH, Wu XH, Zhou Y, Zhang JF. 1,8-Naphthyridine modified naphthalimide derivative: Ratiometric and selective sensor for Hg<sup>2+</sup> in organic aqueous solution. *Bull Kor Chem Soc* 2013;34:63-7.
- [54] Xie P, Xiao Y, Yao D, Jin Q, Guo F. A novel colorimetric and fluorescent "off-on" chemosensor for Cu<sup>2+</sup> based on a rhodamine derivative bearing naphthyridine group. *J Fluoresc* 2013;23:265-71.
- [55] Li Z, Zhao W, Zhang Y, Zhang L, Yu M, Liu J, et al. An 'off-on' fluorescent chemosensor of selectivity to Cr<sup>3+</sup> and its application to MCF-7 cells. *Tetrahedron* 2011;67:7096-100.
- [56] Jin SW, Zhao QJ, Qian XG, Bis(7-amino-2,4-dimethyl-1,8-naphthyridine)dinitratocadmium(II). *Acta Crystallogr Sect E: Struct Rep* 2007;64:54-5.
- [57] Wang RJ, Pu SZ, Liu G, Cui SQ. The effect of the formyl group position upon asymmetric isomeric diarylethenes bearing a naphthalene moiety. *Beilstein J Org Chem* 2012;8:1018-26.
- [58] Arai R, Uemura S, Irie M, Matsuda K. Reversible photoinduced change in molecular ordering

- of diarylethene derivatives at a solution– HOPG interface. *Chem Soc* 2008;130:9371-9.
- [59] Li ZX, Liao LY, Sun W, Xu CH, Zhang C, Fang CJ, et al. Reconfigurable cascade circuit in a photo- and chemical-switchable fluorescent diarylethene derivative. *J Phys Chem C* 2008;112:5190-6.
- [60] Nakashima T, Miyamura K, Sakai T, Kawai T. Photo-, solvent-, and ioncontrolled multichromism of imidazolium-substituted diarylethenes. *Chem Eur J* 2009;15:1977- 84.
- [61] Kobatake S, Uchida K, Tsuchida E, Irie M. Single-crystalline photochromism of diarylethenes: reactivity–structure relationship. *Chem Commun* 2002;2804-5.
- [62] Li WL, Jiao CH, Li X, Xie YH, Nakatani K, Tian, H, et al. Separation of photoactive conformers based on hindered diarylethenes: efficient modulation in photocyclization quantum yields. *Angew Chem Int Ed* 2014;53:4603-7.
- [63] Chen S, Chen LJ, Yang HB, Tian H, Zhu, WH. Light-triggered reversible supramolecular transformations of multi-bisthiénylene hexagons. *J Am Chem Soc* 2012;134: 13596-9.
- [64] Xue YM, Wang RJ, Zheng CH, Liu G, Pu SZ. A new multi-addressable molecular switch based on a photochromic diarylethene with a thieno-imidazole unit. *Tetrahedron Lett* 2016;57:1877-81.
- [65] Kowser Z, Tomiyasu H, Jiang X, Rayhan U, Redshaw C, Yamato T. Solvent effect and fluorescence response of the 7-tert-butylpyrene-dipicolylamine linkage for the selective and sensitive response toward Zn(II) and Cd(II) ions. *New J Chem* 2015;39:4055-62.
- [66] Kobatake S, Yamada T, Uchida K, Kato N, Irie M. Photochromism of 1, 2-Bis (2, 5-dimethyl-3-thienyl) perfluoro-cyclopentene in a single crystalline phase. *J Am Chem Soc* 1999;121: 2380-6.

- [67] Shibata K, Muto K, Kobatake S, Irie M. Photocyclization/cycloreversion quantum yields of diarylethenes in single crystals. *J Phys Chem A* 2002;106:209-14.
- [68] Pu SZ, Tong ZP, Liu G, Wang RJ. Multi-addressable molecular switches based on a new diarylethene salicylal Schiff base derivative. *J Mater Chem C* 2013;1:4726-39.
- [69] Benesi HA, Hildebrand JH. A spectrophotometric investigation of the interaction of iodine with aromatic hydrocarbons. *J Am Chem Soc* 1949;71:2703-7.
- [70] Liu Y, Qiao Q, Zhao M, Yin W, Miao L, Wang L, et al.  $\text{Cd}^{2+}$ -triggered amide tautomerization produces a highly  $\text{Cd}^{2+}$ -selective fluorescent sensor across a wide pH range. *Dyes Pigm* 2016;133:339-44.
- [71] Zhu M, Yuan M, Liu X, Xu J, Lv J, Huang C, et al. Visible near-infrared chemosensor for mercury ion. *Org Lett* 2008;10:1481-4.

**Table Captions:**

**Table 1.** Absorption spectral properties of diarylethenes **1** and **1'** in THF ( $2.0 \times 10^{-5}$  mol L<sup>-1</sup>) at room temperature.

**Table 2.** Truth table of all possible strings of four binary-input data and the corresponding output digit.

**Table 1.**

Compd.	THF		$\Phi^c$		Conversion at PSS in THF
	$\lambda_{o,max}/nm^a$ ( $\epsilon/L mol^{-1} cm^{-1}$ )	$\lambda_{c,max}/nm^b$ ( $\epsilon/L mol^{-1} cm^{-1}$ )	$\Phi_{o-c}$	$\Phi_{c-o}$	
<b>1</b>	331 ( $3.62 \times 10^4$ )	562 ( $9.31 \times 10^3$ )	0.18	0.10	48%
<b>1'</b>	387 ( $9.27 \times 10^3$ )	550 ( $2.81 \times 10^4$ )	0.27	0.005	72%

<sup>a</sup> Absorption maxima of open-ring isomers.

<sup>b</sup> Absorption maxima of closed-ring isomers.

<sup>c</sup> Quantum yields of cyclization reaction ( $\Phi_{o-c}$ ) and cycloreversion reaction ( $\Phi_{c-o}$ ), respectively.

**Table 2.**

Input				Output <sup>a</sup>
In1 (UV)	In2 (Vis)	In3 (Cd <sup>2+</sup> )	In4 (EDTA)	$\lambda_{em} = 541 \text{ nm}$
0	0	0	0	0
1	0	0	0	0
0	1	0	0	0
0	0	1	0	1
0	0	0	1	0
1	1	0	0	0
1	0	1	0	0
1	0	0	1	0
0	1	1	0	1
0	1	0	1	0
0	0	1	1	0
1	1	1	0	1
1	1	0	1	0
1	0	1	1	0
0	1	1	1	0
1	1	1	1	0

<sup>a</sup> At 541 nm, the emission intensity above the original value of **1C**-Cd<sup>2+</sup> (250) is defined as 1, otherwise defined as 0.

**Figure Captions:**

**Scheme 1.** Photochromism of diarylethene **10**.

**Scheme 2.** Synthetic route to diarylethene **10**.

**Scheme 3.** Schematics of molecular structures and fluorescence changes of **10** induced by TBAH / HCl and light stimuli.

**Scheme 4.** Schematics of molecular structures and fluorescence changes of **10** induced by Cd<sup>2+</sup> / EDTA and light stimuli.

**Figure 1.** Absorption spectral and color changes of **1** by photoirradiation in THF ( $C = 2.0 \times 10^{-5}$  mol L<sup>-1</sup>) at room temperature.

**Figure 2.** ORTEP drawing of crystals of **10** (A) and photographs of photochromic for diarylethene **1** (B) in the crystalline phase.

**Figure 3.** Changes in the fluorescence of **10** upon alternating irradiation with UV and visible light in THF ( $C = 2.0 \times 10^{-5}$  mol L<sup>-1</sup>), excited at 360 nm.

**Figure 4.** Absorption spectral changes of **1** induced by TBAH / HCl and light stimuli in THF ( $C = 2.0 \times 10^{-5}$  mol L<sup>-1</sup>) at room temperature: (A) absorption spectral changes of **10** upon addition of TBAH / HCl, (B) absorption spectral changes of **10'** by photoirradiation, (C) absorption spectral changes of **1C** upon addition of TBAH / HCl.

**Figure 5.** Changes in the fluorescence changes of **1** induced by TBAH / HCl and light stimuli in THF ( $C = 2.0 \times 10^{-5}$  mol L<sup>-1</sup>) at room temperature, excited at 650 nm: (A) **10'** induced by photoirradiation.

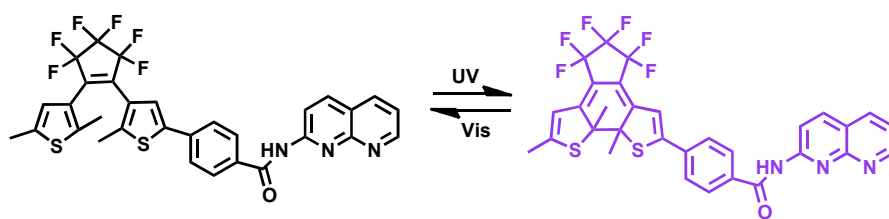
**Figure 6.** Changes in the fluorescence of **10** induced by the addition of various metal ions (3.0 equiv) in THF ( $C = 2.0 \times 10^{-5}$  mol L<sup>-1</sup>): (A) emission spectral changes, (B) emission intensity

changes, (C) photos demonstrating changes in its fluorescence.

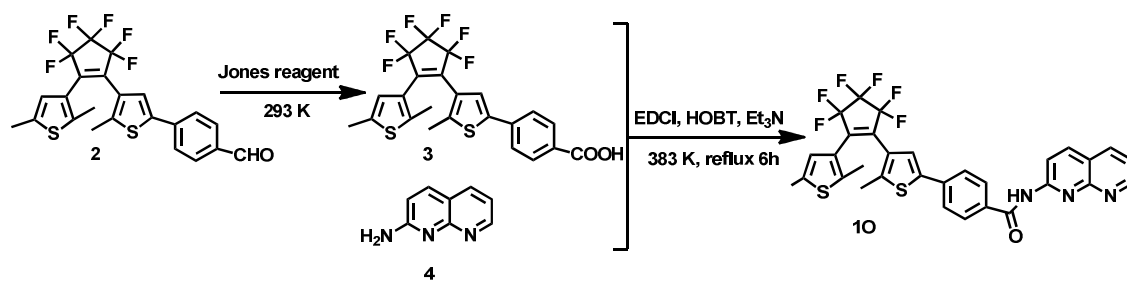
**Figure 7.** Emission spectral changes of **10** induced by  $\text{Cd}^{2+}$  / EDTA and light stimuli in THF ( $C = 2.0 \times 10^{-5} \text{ mol L}^{-1}$ ) at room temperature, excited at 360 nm: (A) **10** induced by  $\text{Cd}^{2+}$  / EDTA, (B) emission intensity changes of **10**- $\text{Cd}^{2+}$  by alternating irradiation with UV / vis light.

**Figure 8.** (A) Competitive tests for the fluorescent responses of **10** to various metal ions in THF: Red bars represent the addition of 3.0 equiv of various metal ions to the solution of **10**, Black bars represent the addition of  $\text{Cd}^{2+}$  (3.0 equiv) to the above solution, (B) Job's plot showing the 1:1 complex between **10** and  $\text{Cd}^{2+}$ , and (C) The  $^1\text{H}$  NMR spectrum changes of **1** by addition of  $\text{Cd}^{2+}$  solution in  $\text{THF-}d_8$ .

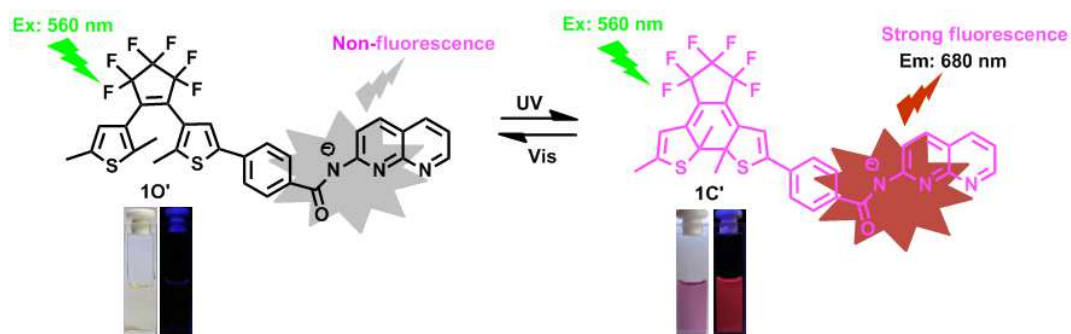
**Figure 9.** The combinational logic circuit equivalent to the truth table given in Table 1: In1 (297 nm light), In2 (500 nm visible light), In3 ( $\text{Cd}^{2+}$ ), In4 (EDTA) and O (Output signal).



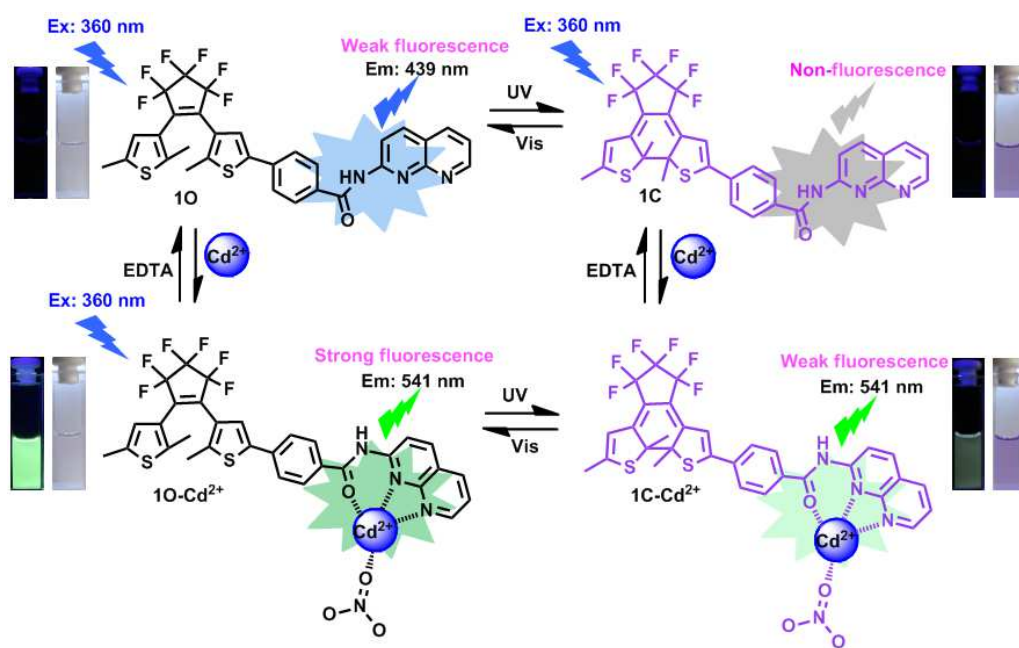
Scheme 1



Scheme 2



Scheme 3



Scheme 4

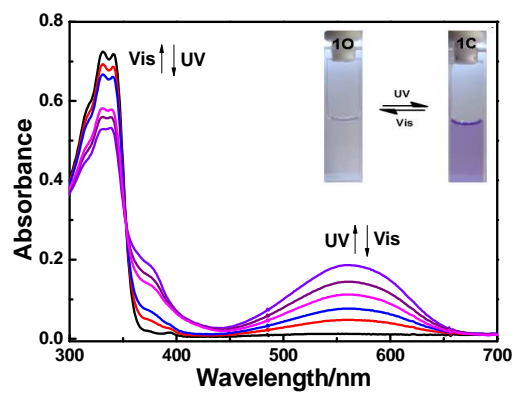
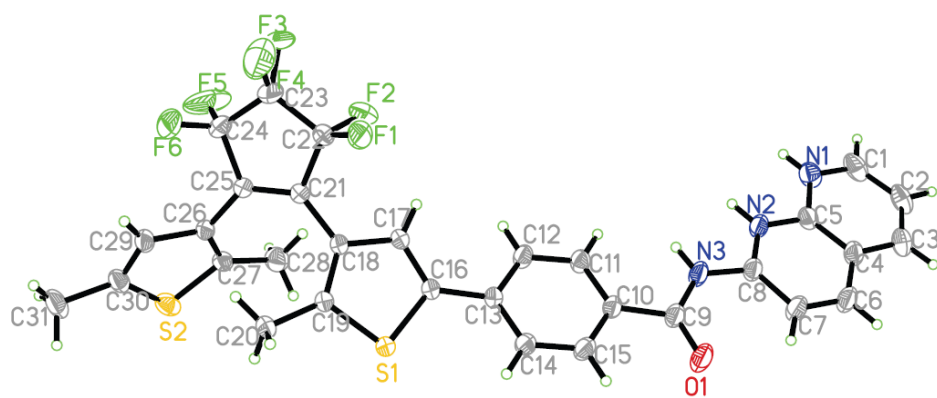
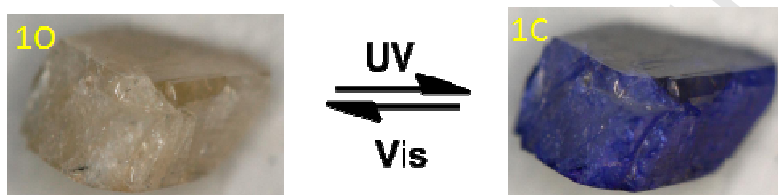


Figure 1



(A)



(B)

Figure 2

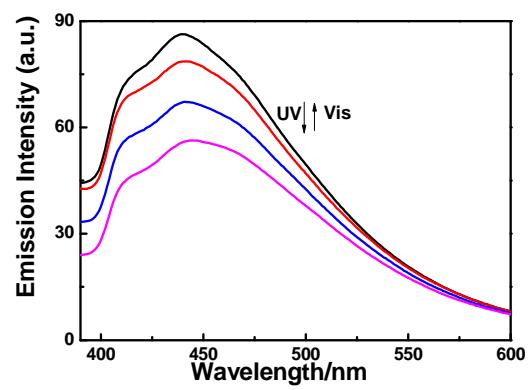


Figure 3.

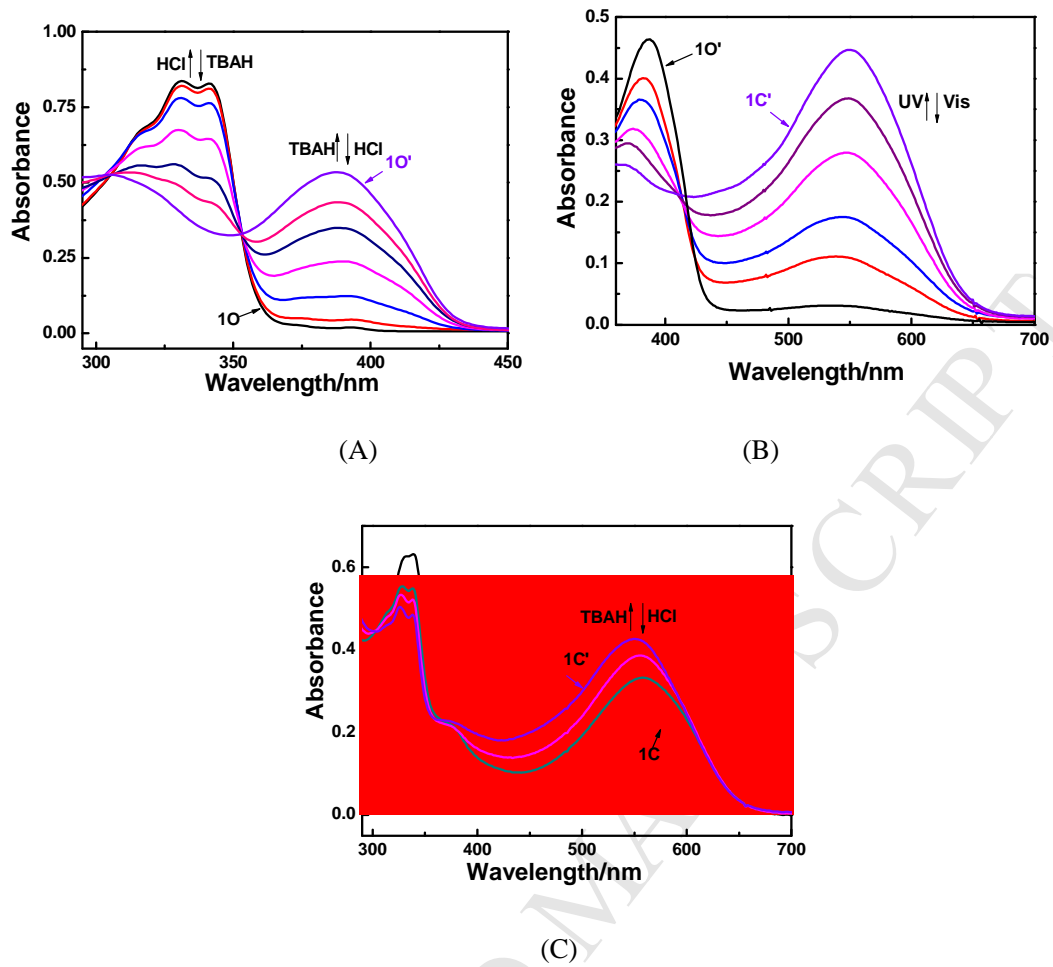


Figure 4

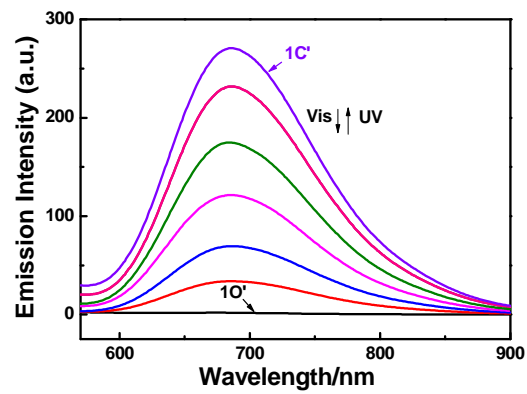


Figure 5

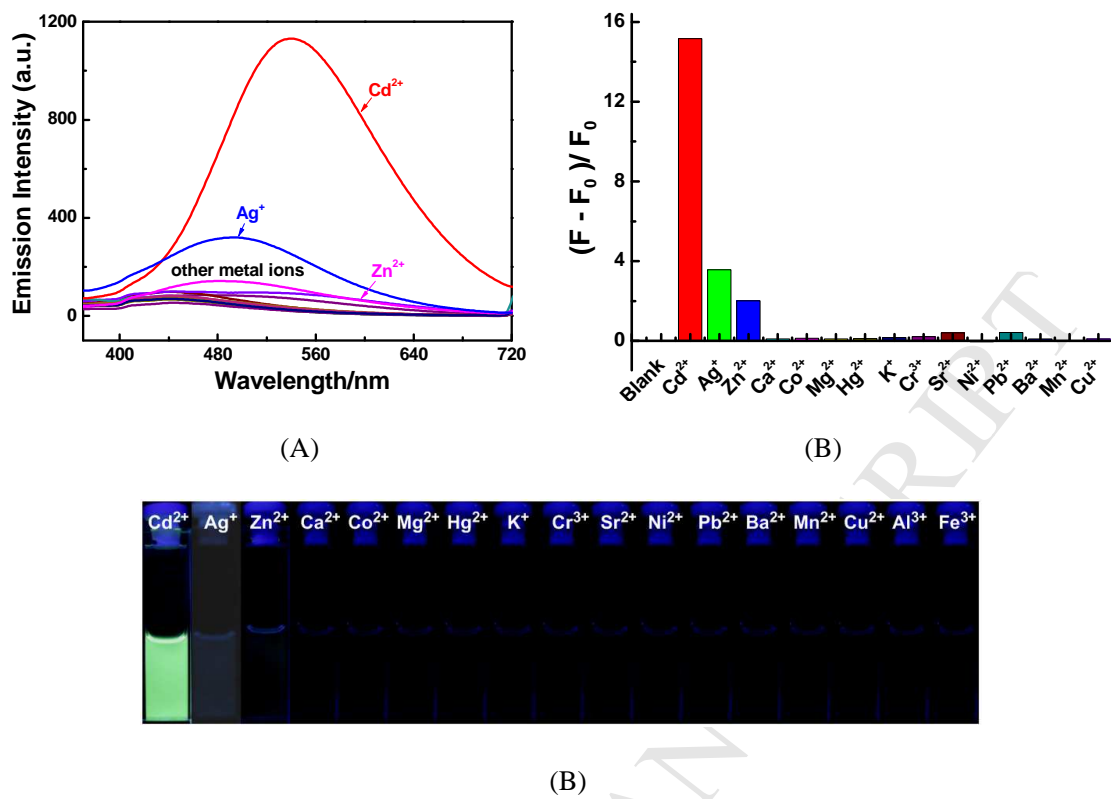


Figure 6

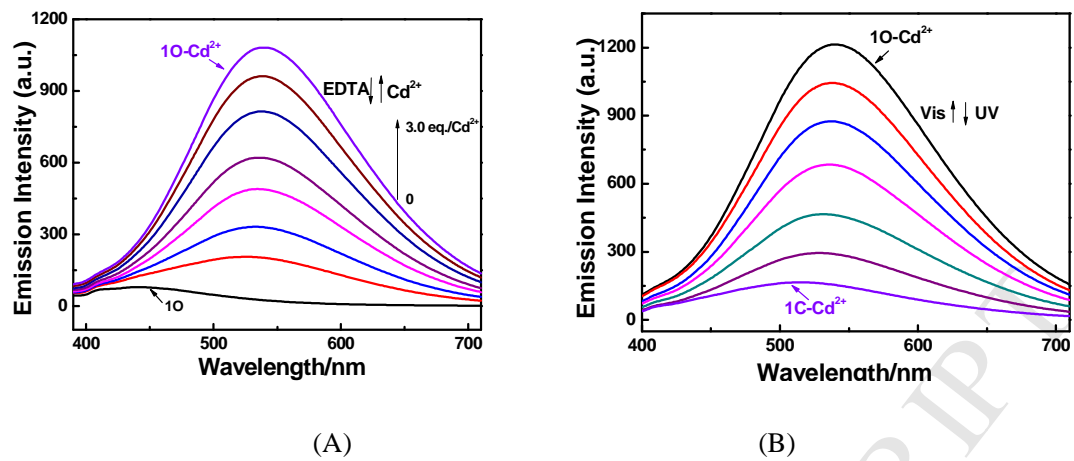
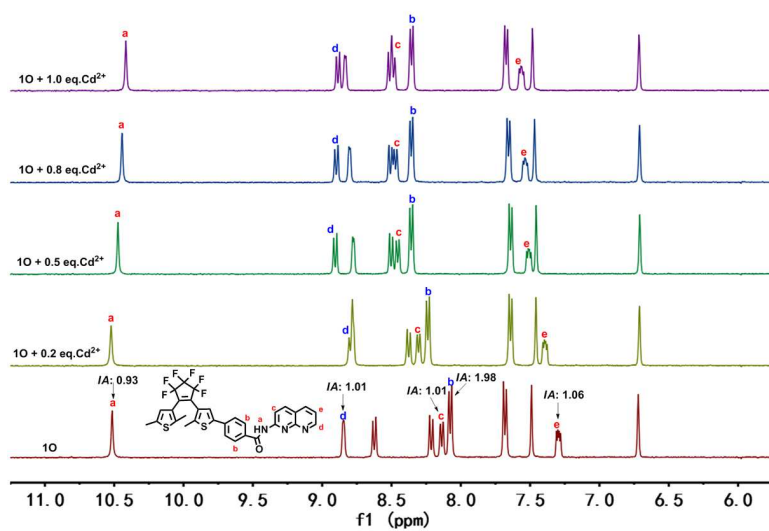
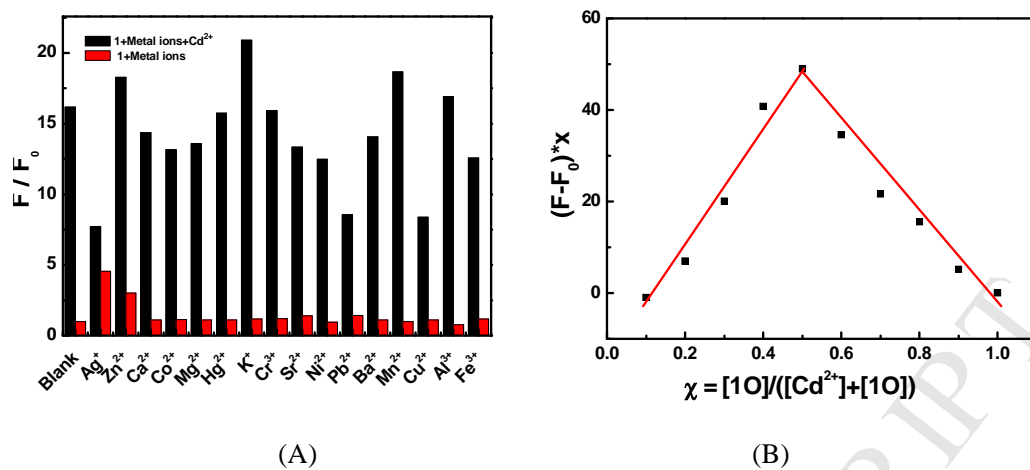


Figure 7



(C)

Figure 8

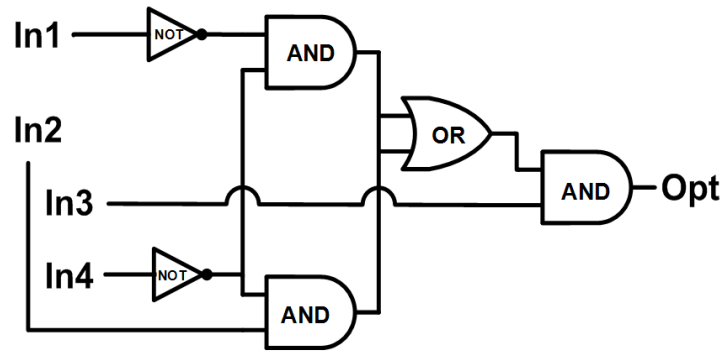


Figure 9

## Highlights

- A new diarylethene with an 1,8-naphthyridine unit was synthesized > Its fluorescence could be efficiently modulated by light, base/acid, and metal ion > It was highly selective toward  $\text{Cd}^{2+}$  with an obvious fluorescent color change from dark to green